CHAPTER 2

^{1}H-NMR Determination of Base Pair Lifetimes in Oligonucleotides Containing Single Base Mismatches

Adapted from Bhattacharya, P. K., Cha, J., Barton, J. K. (2002) *Nucleic Acids Research, 30,* 4740-4750.

Abstract

Proton nuclear magnetic resonance (NMR) spectroscopy is employed to characterize the kinetics of base-pair opening in a series of nine-mer duplexes containing different single base mismatches. The imino protons from the different mismatched as well as fully matched duplexes are assigned from the imino-imino region in the WATERGATE NOESY spectra. The exchange kinetics of the imino protons are measured from selective longitudinal relaxation times. In the limit of infinite exchange catalyst concentration, the exchange times of the mismatch imino protons extrapolate to much shorter lifetimes than commonly observed for an isolated GC base pair. Different mismatches exhibit different orders of base-pair lifetimes, *e.g.* a TT mismatch has a shorter base-pair lifetime than a GG mismatch. The effect of the mismatch was observed up to a distance of two neighboring base pairs. This indicates that disruption in the duplex caused by the mismatch is quite localized. The overall order of base-pair lifetimes in the selected sequence context of the base pair is GC > GG > AA > CC > AT > TT. Interestingly, the fully matched AT base-pair has a shorter base-pair lifetime relative to many of the mismatches. Thus, in any given base pair, the exchange lifetime can exhibit a strong dependence on sequence context. These findings may be relevant to the way mismatch recognition is accomplished by proteins and small molecules.

Introduction

DNA mismatches, or non-complementary base-pairs, arise *in vivo* as a result of the misincorporation of bases during replication (1), heteroduplex formation during homologous recombination (2), mutagenic chemicals (3, 4), ionizing radiation (5), and spontaneous deamination (6). These errors are usually detected and eliminated by DNA polymerase and postreplicative mismatch repair system (7-9). How these DNA mismatches are detected by the repair machinery of the cell requires an understanding at the molecular level. Therefore, it is useful to characterize the structure, dynamics, and biochemistry of various mismatched base pairs in DNA and to determine how they affect the structure of the double helix both in terms of global and local perspective.

The structures of several DNA duplexes containing mismatched base pairs have been characterized by x-ray crystallography (10-12) and NMR methods (13-16). In all of these structural studies, the mismatches are shown to have minimal effect on the global conformation of the DNA; the distortions produced are limited to the mismatched site and neighboring base pairs. ^{1}H NMR studies show that the mismatches GG (17-19), AA (20-22), TT (20-22), CC (23, 24), GA (25-28) and GT (29), are well stacked in the helix and the bases remain in an intrahelix orientation. In fully base paired right-handed B-form DNA duplexes, there are NOE's evident between base protons (H8 or H6) and the 5'-flanking sugar H1' and H2'2" protons, allowing an NOE walk from the 5' to the 3'-end of the oligonucleotide. In the case of these mismatched duplexes, the NOE walk is conserved, again supporting the notion that the mismatches are inserted and stacked well between the flanking base-pairs and the oligonucleotides adopt the classical B form duplex with minimal local disruption. Additionally, ^{31}P NMR studies support a B_1 conformation (17, 19, 20, 23).

Much less is known about the dynamical properties of the mismatched bases in the DNA duplex and about any possible role of dynamics in mismatch recognition. The bases in DNA move rapidly within the double helix, undergoing thermally driven

structural fluctuations in solution. Since base motions occur within a multidimensional potential well, determined by a combination of base-stacking and base-pairing forces, it is reasonable to expect that the motions of a mismatched base pair in DNA should be different from that of the fully matched pair; this dynamical difference may influence the interactions of mismatched base pairs with repair enzymes. Furthermore, the dynamics of mismatches as well as fully matched base pairs may play a pivotal role in modulating charge transport through DNA, which is a topic of considerable current interest (30-38).

The dynamics of mismatched duplexes has been the focus of spectroscopic studies by Millar *et al* (39). Time resolved fluorescence anisotropic decay measurements were obtained for a series of oligonucleotides containing intervening AP•X base-pairs, where AP is the fluorescent adenine analogue, 2-aminopurine, and X=A, T, G and C. This technique allowed the detection of base motions in DNA on the picosecond time scale. Motions such as helical twisting, propellar twisting, base tilting and base rolling could potentially alter the emission dipole of AP, thereby contributing to changes in the decay of the fluorescence anisotropy. AP pairs differently with each of the different bases and these differences in its relative pairing ability were reflected in the internal dynamics.

A complementary method of probing base pair dynamics is through ^{1}H NMR studies of imino proton exchange rates. Clearly, such studies probe base pair motions on a much slower time scale. The imino protons of the aromatic heterocyclic base exchange with the solvent protons when the hydrogen bond in the base pair is disrupted (41, 42). The chemical proton transfer step from the open state is usually rate limiting, and a proton acceptor, the base catalyst, must be added to solution in order to accelerate the exchange close to opening-limited conditions. Base pair lifetimes are then obtained by extrapolation of the exchange times to infinite catalyst concentration, where the dissociation constant of a base pair is estimated by comparing the exchange rates of the imino proton in the base pair and in the mononucleoside. The unknown factor in this comparison is the accessibility of the imino proton in the open base pair, which is related

to properties of the open state. Measurements of the NMR relaxation rates of the imino protons as a function of solvent exchange have yielded lifetimes in the range 1-40 ms for fully paired bases in B-DNA (43). In general, AT base-pair lifetimes have been found to be in the range 1-5 ms at 15 °C, except for AT tracts where lifetimes longer than 100 ms have been observed (44). For GC base pairs, lifetimes about 10 times longer than for AT base-pairs have been observed (43), as one might expect, given the presence of an additional hydrogen bond in the GC base pair. However, it is important to note that the sequence composition (44, 45), the charged state of the double helix (46), and drug interactions (47) all serve to modulate base-pair dynamics sensitively.

Here we report a systematic study of the dynamics of single base mismatches within DNA duplexes through the measurements of imino proton exchange. Using ^{1}H NMR, we have determined the base pair lifetimes of different mismatches in a given sequence context and have compared the exchange times with those of fully matched base pairs. We observe strong sequence dependence of the base-pair opening times and that rates are increased at the mismatched site and in the directly neighboring site. These results underscore the importance of DNA sequence and of sequence context in governing base dynamics.

Experimental

Oligonucleotide Preparation. Oligonucleotides were synthesized using standard phosphoramidite chemistry on an Applied Biosystems 392 DNA synthesizer with a dimethoxy trityl protecting group on the 5'end (48). Oligonucleotides were purified on a reversed-phase Rainin Dynamax C_{18} column on a Waters HPLC and then deprotected by incubation in 80% acetic acid for 15 minutes. After deprotection, the oligonucleotides were purified again by HPLC. Following purification, these oligonucleotides were desalted on a Waters C_{18} SepPak column and then converted to a sodium salt using CM Sephadex C-25 (Sigma) equilibrated in NaCl. The concentration of the oligonucleotides

was determined by UV-visible spectroscopy (Beckman DU 7400) using the extinction coefficients estimated for single-stranded DNA: ε(260 nm, $M^{-1}cm^{-1}$) adenine (A) = 15,400; guanine (G) = 11,500; cytosine (C) = 7,400 and thymine (T) = 8,700. Single strands were mixed with equimolar amounts of complementary strand and annealed using a Perkin Elmer Cetus Thermal Cycler by gradual cooling from 90°C to ambient temperature in 90 minutes. The NMR samples were prepared by dissolving the oligonucleotides in a buffer solution (5 mM Na_2HPO_4, 15 mM NaCl, pH 7.0). The concentrations of the samples varied between 0.5-1.2 mM duplex.

Melting Temperature Experiments. The melting temperatures of the oligonucleotides were determined from absorbance versus temperature curves measured at 260 nm on a Beckman DU 7400 UV-visible spectrophotometer. 10 μM duplex was used in a buffer of 5 mM Na_2HPO_4, 15 mM NaCl, pH 7.0. The melting profile of the duplexes were obtained by slowly lowering the temperature (0.5 °C per minute) from 75 °C to 10 °C and measuring the absorbance at 260 nm at each temperature. The T_m values represent the midpoint of the transition as obtained by fitting the melting profiles with a sigmoidal expression in Origin.

NMR Spectroscopy. One and two dimensional ^1H NMR spectra were taken in both D_2O and 90/10 H_2O/D_2O at 277 K on a Varian INOVA 600 MHz spectrometer. For the spectra taken in 90/10 H_2O/D_2O, WATERGATE gradient pulse water suppression (49) was used. The conditions of acquiring the spectra were: 600 MHz, 20 ppm sweep width, TPPI, 2048 complex points, hypercomplex mode, 256 t_1 blocks, 64 scans per t_1 block, 1.3 s relaxation delay, 120 ms mixing time. ROESY spectra (50, 51) were obtained at variable mixing times of 80, 150 and 300 ms keeping the other parameters the same as for the WATERGATE NOESY experiments with the r.f. strength for the spin-lock field set at 3.5 kHz. Linear prediction was employed in the indirect dimension to increase resolution close to the diagonal. All two dimensional processing was carried out with

VNMR 6.1b software (Varian) on a SUN workstation. Chemical shifts were reported relative to the internal standard, sodium 3-trimethylsilyl-[2,2,3,3-D_4] propionate (TMSP).

Imino Proton Exchange Measurements. Imino proton exchange within the DNA duplex occurs through the opening of the base pair followed by exchange from the open state. The conformational features of this state are not yet fully understood. To account for proton exchange data, it is generally assumed that, in the open state, the imino groups are fully accessible to solvent and the base-pairing hydrogen bonds are broken such that the imino proton becomes available for hydrogen bonding with water or catalyst molecules (41). The chemical proton transfer step from the open state is rate limiting, and a proton acceptor like OH^- must be added to accelerate the exchange close to opening-limited conditions. The base-pair lifetimes are obtained by extrapolation of the exchange times to infinite base catalyst concentration.

$$k_{ex} = \Sigma_n k^n_{op}\, k^i_{tr}[B]/\, k^n_{cl}/\alpha^n + k^i_{tr}[B]$$

For a base-pair with multiple open states, formed with rates k^n_{op} and closed with rates k^n_{cl}, and provided that $\Sigma_n k^n_{op} \ll k^1_{cl}, k^2_{cl}, \ldots, k^n_{cl}$, the total imino proton exchange rate k_{ex} equals the sum of the exchange rates from each mode (41). To simplify, where k^i_{tr} is, as above, the intrinsic imino proton-transfer rate from the mononucleoside and α^n is a parameter reflecting the different accessibility of the imino proton in the open states and in the mononucleoside and [B] denotes the concentration of the exchange catalyst, OH^- in this case, then for a base pair with a single opening mode (n = 1) and with $k_{op} \ll k_{cl}$, this can be written as:

$$\tau_{ex} = \tau_{op} + 1/\alpha K_d k_{tr}^{i}[B] \qquad (1)$$

where τ_{ex} and τ_{op} are the inverse exchange and opening rate, respectively, and $K_d = k_{op}/k_{cl}$ is the base-pair dissociation constant. A plot of τ_{ex} versus 1/[B] yields a straight line where τ_{op} is obtained from the y-axis intercept and αK_d from the slope. The limit where Equation 1 is valid is known as Linderstrøm-Lang kinetics (52).

In this work, the oligonucleotides were titrated using ammonia (4 M ammonia buffer, 1.25 M ammonium chloride, pH 10.0; Ricca Chemical Co.) as the exchange catalyst. The oligonucleotide concentrations of the samples varied between 0.5-1.2 mM duplex, and the oligo sample was buffered with 5 mM Na_2HPO_4, 15 mM NaCl, pH 7.0. The imino proton exchange times (τ_{ex}) at different catalyst concentrations, were obtained from measurements of the inversion recovery times in the presence (T_{rec}) and absence (T_{aac}) of exchange catalyst according to the equation

$$1/\tau_{ex}=1/T_{rec} - 1/T_{aac} \qquad (2)$$

Except for longitudinal dipolar relaxation, direct exchange to water as well as exchange catalyzed by OH^- ions and the acceptor nitrogen of the opposite base contributes to the recovery rate of the imino protons in the absence of added catalyst $1/T_{aac}$. However, these contributions remain constant when the catalyst is added and will be canceled in Equation 2. Consequently, the exchange time τ_{ex} represents exchange only via the added catalyst. Thus, the NMR measurable in the whole series of the base-pair lifetimes experiments is T_1, the longitudinal relaxation time. Essentially, we are measuring the T_1 values for various imino protons and of course, the effect of the exchange catalyst on T_1.

The experiment was carried out by creating a designed pulse sequence comprised of a 3.2 ms 180˚ Gaussian pulse(g3) for selective inversion, a variable delay, and a 5 ms 90˚ Gaussian observe pulse(g4). Right shift and linear prediction of the free induction decay are employed to correct for magnetization evolution during the observed pulse. The carrier frequency was centered on the imino proton region. The spectral width was 7000 Hz and the experiments were carried out at 600 MHz.

Results and Discussion

Sequence Design. The general nine-mer oligonucleotide sequence $d(GACA\mathbf{X}TGTC)_2$; where **X**= G, T, A, C, was employed to determine the base-pair lifetimes for DNA duplexes containing different central single base mismatches (Table 1)

Table 2.1. The Sequences and the Melting Temperatures (T_m) of the Duplexes Containing a Single Base Mismatch (XY) Used in the NMR Experiments.

Duplexes[a]	T_m (°C)[b]
5′GACA**G**TGTC3′ 3′CTGT**G**ACAG5′	34.9
5′GACA**C**TGTC3′ 3′CTGT**C**ACAG5′	24.5
5′GACA**A**TGTC3′ 3′CTGT**A**ACAG5′	32.1
5′GACA**T**TGTC3′ 3′CTGT**T**ACAG5′	32.4
5′GACA**G**TGTC3′ 3′CTGT**C**ACAG5′	47.8
5′GACA**A**TGTC3′ 3′CTGT**T**ACAG5'	44.1

[a]These sequences represent the six oligonucleotides employed for the imino exchange experiments. The single base mismatched or matched base-pairs are highlighted in bold.
[b]Shown are the melting temperatures (T_m) of the duplexes determined as described in the Experimental section. Samples include 10 μM duplex in a buffer of 5 mM Na_2HPO_4, 15 mM NaCl, pH 7.0. The order of the melting temperature varies as: GC > AT > GG > TT ~ AA > CC

A palindromic sequence was utilized that is self-complementary except at the mismatch site (X). This simplifies the ^{1}H NMR spectra and facilitates the assignment of the protons. Table 1 also shows the melting temperatures for the different duplexes and demonstrates that duplexes containing mismatches are thermodynamically destabilized as compared to the matched pairs.

For the mismatched duplexes, only one strand was used resulting in a duplex with either AA, TT, CC or GG mismatch at the central site (X); to obtain a complementary base-pair at site X, however, two different strands had to be used. This fact led to the possibility of the formation of a mixture of matched and mismatched duplexes as two separate strands were added to form the fully matched GC and AT sequences. Given the melting temperatures, that possibility was minimized by slow cooling during hybridization of the duplexes and repeated annealing of the sample to allow nucleation. In the case of the AT-matched duplex, no resonances corresponding to the imino protons of mismatched base-pairs were observed. For the GC matched duplex only a small fraction was observed (*vide infra*), confirming the isolation of duplexes with primarily Watson-Crick base pairs. The nine-mer duplex was also chosen in part to preserve the sequence used in guanine oxidation studies reported elsewhere (38). The possibility of hairpin formation is negligible with 9-mer duplexes. Moreover, non-denaturing agarose gel electrophoresis with the mismatch-containing duplexes indicated no formation of hairpins in these duplexes (data not shown).

Imino Proton Resonance Assignment. The imino proton resonances of the different oligonucleotides were assigned primarily from the imino-imino crosspeaks in the WATERGATE NOESY spectra in 90:10 H_2O/ D_2O solution (Table 2). The B-form structure of the DNA duplex constrains the position of imino protons in the duplex to be 3.4 Å above or below one another; in the fully matched duplex, each base pair contains one imino proton (N_3H in thymine and N_1H in guanine). These interactions between the imino protons lead to crosspeaks in the imino-imino region of the two dimensional

1 2 3 4 5 6 7 8 9

5′-GACA**X**TGTC-3′ where **X** / **Y**= A, T, G, C

3′-CTGT**Y**ACAG-5′

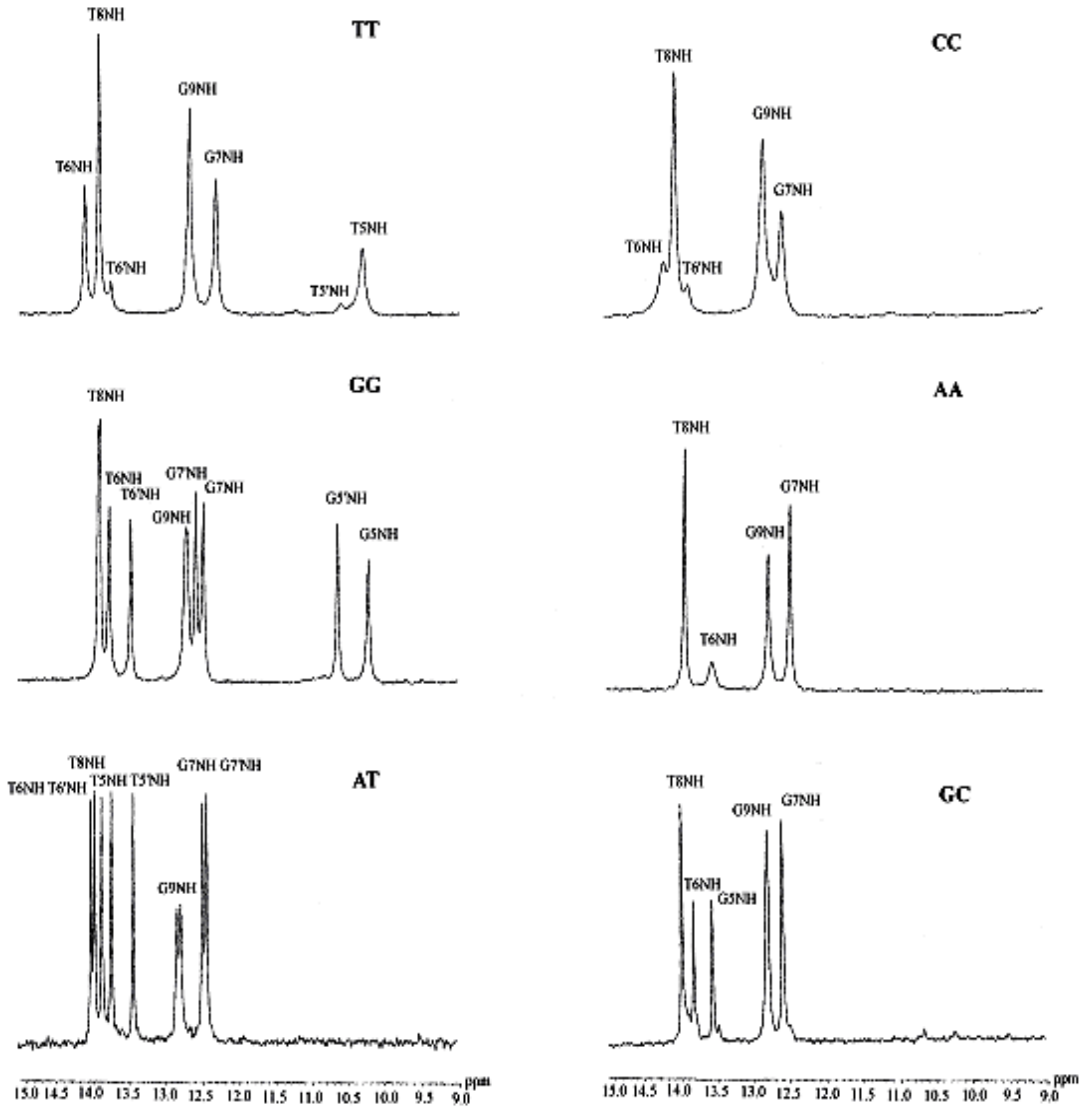

Figure 2.1. One dimensional ^{1}H NMR spectra of the exchangeable imino region (9-15 ppm) of the oligonucleotides with intervening GG, TT, AA ,CC mismatches and the fully matched AT and GC base pairs at 600 MHz. Samples contained 0.5-1.2 mM oligonucleotides, 5 mM Na_2HPO_4 and 15 mM NaCl buffer at pH 7.0 in 90:10 H_2O/D_2O at 277 K. The peaks are assigned from the respective imino-imino region of the two dimensional NOESY spectra. Chemical shifts are reported relative to TMSP (0.00 ppm). The chemical shifts of the individual imino resonances in all the duplexes are given in Table 2.

Table 2.2. The Chemical Shifts[a] (ppm) of the Iimino Proton Resonances in the Oligonucleotides Containing the Intervening Mismatches (XY).

```
    1 2 3 4 5 6 7 8 9
5′-GACAXTGTC-3′  where X, Y= A, T, G, C
3′-CTGTYACAG-5′
```

[b]Base pairs	X/Y5NH[c] (ppm)	T6NH[d] (ppm)	G7NH[d] (ppm)	T8NH[d] (ppm)	G9NH[d] (ppm)
G•G	10.65 10.22	13.76 13.46	12.70 12.47	13.92 13.89	12.71
T•T	10.72 10.41(sm)	14.25 13.87(sm)	12.44	14.03	12.79
C•C	-----	14.20 13.87(sm)	12.54	14.04	12.80
A•A	-----	13.55	12.46	13.92	12.76
G•C*[e]	13.54	13.81	12.57	13.97	12.78
A•T*[e]	13.72 13.42	14.01 13.96	12.47 12.41	13.85	12.79

[a]Samples for NMR studies are prepared as described in the Experimental section and the proton chemical shifts are relative to TMSP (0.00 ppm). The samples were at a concentration of 0.5-1.2 mM duplex and taken in a buffer solution of 5 mM Na_2HPO_4, 15 mM NaCl, pH 7.0 in 90:10 H_2O/D_2O. [b]Designation of XY as shown in assembly. [c]The imino proton attached to the central mismatched base pair is denoted by X/Y5NH. The assignment of the imino protons was accomplished from the imino-imino cross peaks of the WATERGATE NOESY spectra of the oligonucleotides in 90:10 H_2O/ D_2O as described in the Results & Discussion section. [d]Because of the symmetry of the duplexes and the fact that each base-pair can have only one imino proton (expect the mismatched pairs), imino protons at G1, T2, G3 and T4 sites are usually equivalent to that of G9, T8, G7 and T6 respectively. The presence of the two values of the chemical shift reflects the loss of this symmetry. [e]XY* corresponds to the Watson-Crick paired sequence.

NOESY spectra of the DNA duplexes, which can be exploited for the assignments of these protons.

Figure 1 shows the exchangeable imino region (9-15 ppm) of the one-dimensional ^{1}H NMR spectrum for sequences containing GG, AA, TT, CC mismatches and for the fully matched sequences containing AT and GC base pairs. For all of the oligonucleotides under study, one observes three main sets of imino protons: a) thymine imino protons in the range of 14.3-13.4 ppm, b) guanine imino protons mostly in the range of 12.8-12.4 ppm and c) a set of imino protons from the mismatched sites (GG & TT) in the range of 10.2-10.7 ppm. These shifted resonances at the mismatch site are more exposed and subject to exchange with solvent than those of the stacked base pairs. Nonetheless, most of the imino protons are quite well resolved. As is evident in Table 2, for all of the duplexes, the chemical shifts of the outer imino protons ($G9N_1H$, $T8N_3H$ and $G7N_1H$) remain quite close to each other. This similarity in chemical shift is consistent with previous observations that perturbations caused by the mismatches are localized, limited essentially to the flanking bases (10-12).

The linewidths of the imino proton(s) for the different duplexes containing mismatches clearly differ depending upon the base composition of the mismatch. TT and CC mismatch-containing duplexes exhibit larger linewidths as compared to GG and AA duplexes. This variation in linewidth correlates with the relative stability of the duplexes; such broad linewidths for duplexes containing TT and CC mismatches have also been seen previously (24).

A representative imino-imino region in the NOESY spectra of the duplex containing a GG mismatch is shown in Figure 2. Since the imino protons are stacked one above another, the interactions among them lead to a NOE walk of the imino-imino cross peaks along the length of the oligonucleotide. Furthermore, the two imino protons from the mismatched guanine (GG) base-pair are positioned at a close proximity to each other and exhibit a strong NOE build up between them (G5/G5’). The peak splitting for the G5

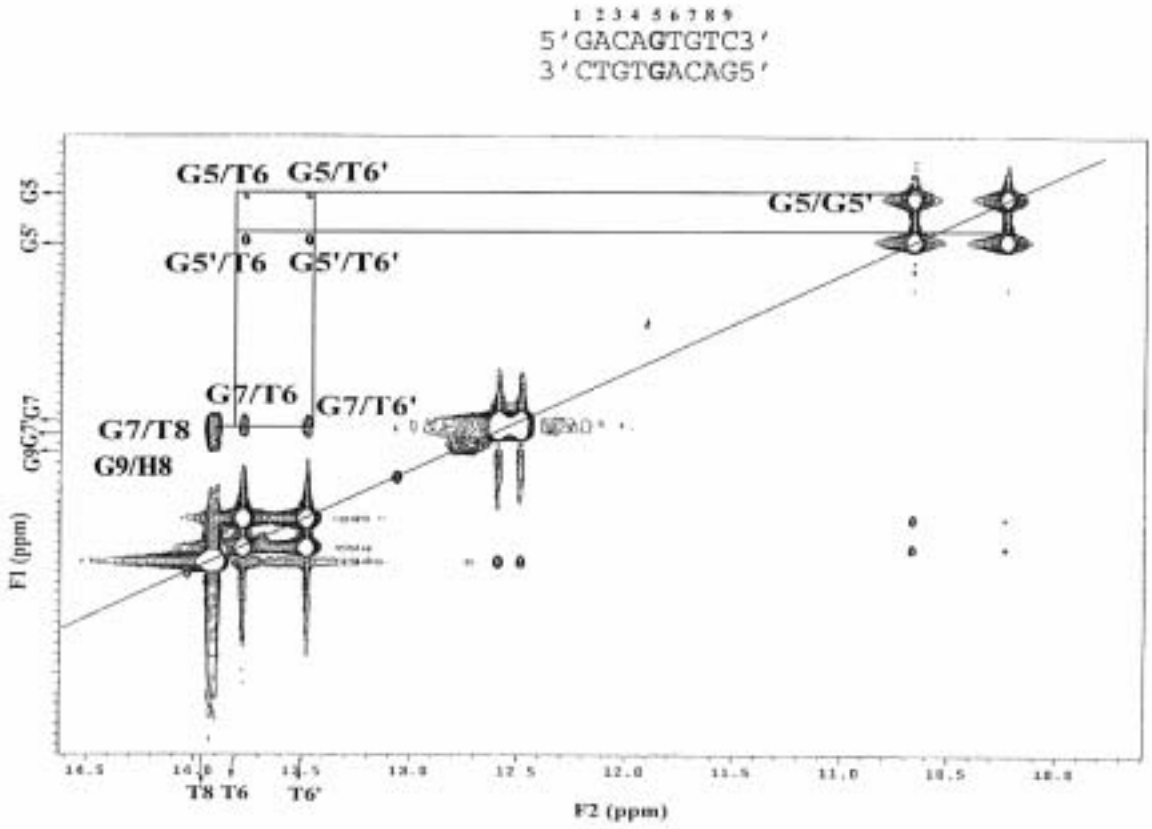

Figure 2.2. Expanded imino-imino region of the two dimensional NOESY contours in 90:10 H_2O/D_2O for the duplex d(GACAGTGTC)$_2$ containing an intervening GG mismatch. Solution is 1 mM in DNA duplex, 5 mM Na_2HPO_4 and 15 mM NaCl buffer at pH 7.0. Spectrum is acquired with a mixing time of 120 ms and at 277 K and collected at 600 MHz. The details of the NOESY experiment are outlined in the Experimental Section. Chemical shifts are reported relative to TMSP (0.00 ppm). The lines illustrate the NOE walk along the imino protons which are stacked above or below one another (at a distance of 3.4 Å) along the oligonucleotide.

imino proton reflects an asymmetry in conformation for the two G's at the mismatch site. One G of the GG mismatch has been seen to adopt the *syn* conformation with the alternate G in the *anti*-form, with slow exchange on the NMR time scale (17-19). This asymmetry at the mismatch site extends out to other sites within the duplex; peak splitting is observed not only for G5, but also for T6 and G7 imino resonances. These peaks can easily be assigned from the NOESY spectra.

The TT mismatch is known to be in intermediate exchange between two asymmetric wobble structures involving two imino to carbonyl hydrogen bonds (20-22), and we also observe two peaks for T5 with a faster rate of exchange. Note that one of the T5 peaks is much bigger than the other (T5') indicating the one of the conformations exchange with water at a faster rate relative to the other. For the TT mismatch-containing duplex, the asymmetry can be seen to a small extent on T6. Interestingly, for the CC mismatch-containing duplex, a similar asymmetry is evident in the shifts for T6; since the CC-mismatch lacks imino protons, no asymmetry can be detected directly at the mismatch site. This has been further corroborated by the presence of a crosspeak for the T6N_3H proton in the same phase as the diagonal peak in the two dimensional ROESY spectra of the TT and CC-duplexes (data not shown), which indicates chemical exchange involving that imino proton. A combination of NOESY and ROESY spectra can thus be used to distinguish between cross-relaxation and chemical exchange (50). Note that our assignments of the imino protons of the GG and TT pair are in close agreement with those observed for related nine-mers containing GG and TT mispairs (24).

The one dimensional spectrum for the AA mismatch-containing duplex is relatively simple and is also easily assigned from the imino-imino NOESY spectra. Only four resonances from the four matched base pairs are evident. This observation must reflect a primarily symmetric positioning of the A's within the mismatch site.

Also shown are the one-dimensional spectra for the fully matched duplexes. For the GC-duplex, the G5 imino is now revealed at the expected shift for a matched base

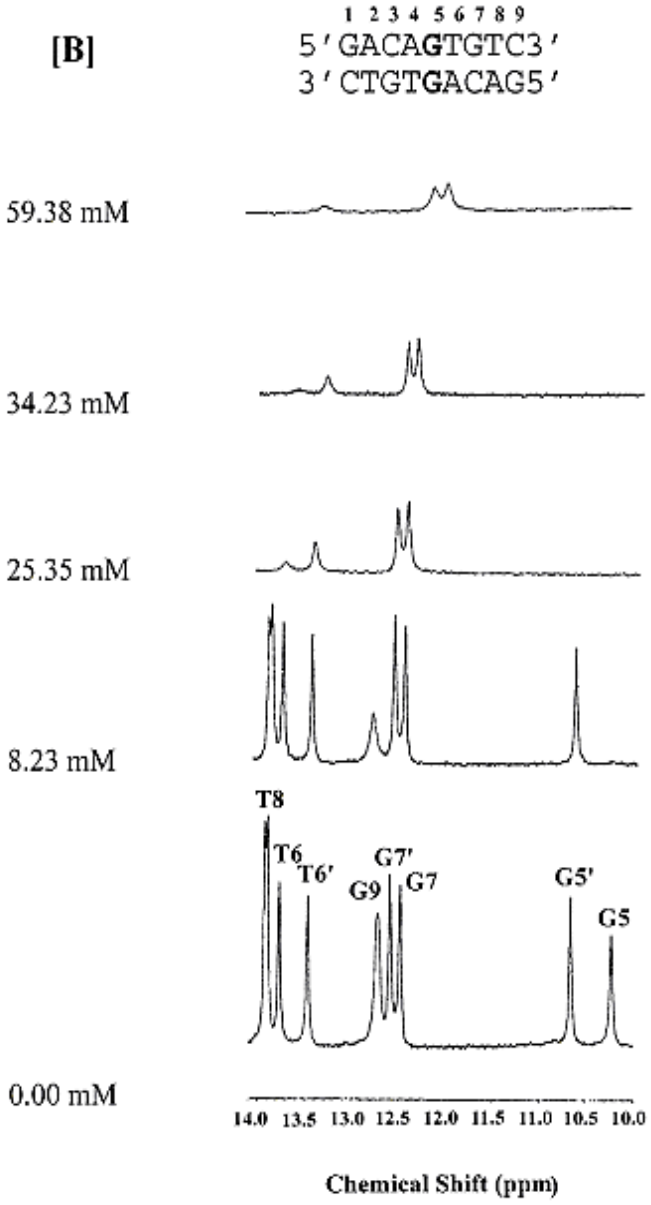

Figure 2.3. The titration of 1mM d(GACAGTGTC)$_2$ with 4 M ammonia buffer in 90:10 H_2O/D_2O followed by ^1H NMR. Shown is the imino proton region of the spectra taken at 600 MHz and 277 K. Conditions are 1 mM in DNA duplex, 5 mM Na_2HPO_4 and 15mM NaCl buffer and 4 M in the titrant Ammonia buffer. Chemical shifts are reported relative to TMSP (0.00 ppm). [B] denotes the concentration of the ammonia buffer in the sample solution at different points of the titration.

pair. In the case of the GC duplex, there are also very small peaks evident at 13.46, 10.65 and 10.22 ppm; we attribute these to the formation of a very small amount of GG mismatch-containing duplex during the hybridization process. Interestingly, sharper resonances are evident for the AT matched oligomer compared to the GC matched duplex. In addition, in the case of the AT matched duplex, peak doubling is evident for most of the resonances, consistent with the symmetry breaking by the TA base pair at the central site. Only one resonance at each position is apparent for the matched GC oligomer; perhaps this results from a more central positioning of the $G5N_1H$ within the duplex.

Imino Proton Exchange. The exchange times of the imino protons were obtained through the measurement of the inversion recovery times of the NMR resonances. The addition of an exchange catalyst, NH_3, yields, in the limit of infinite catalyst concentration, the kinetic parameters for the base-pair opening (Equation 1). Upon titration with base, the general observation was broadening and the gradual disappearance of the imino proton resonances as the exchanges times became too fast to be observed on the NMR time scale. Figure 3 shows the variation in the one dimensional spectrum for the GG mismatch-containing duplex as a function of increased base concentration. Different imino protons are seen to broaden out at differing levels of base concentration. For example, $G7N_1H$ and $T6N_3H$ broaden out at a much slower rate compared to the imino protons G9 and G5. This is consistent with the fact that the outermost protons ($G9N_1H$ and $T8N_3H$) as well as the protons at the mismatch site ($G5N_1H$) are undergoing exchange with solvent at a faster rate than the other internally positioned imino protons and hence the fast relaxation is observed. The linewidth of the $G9N_1H$ imino proton is relatively broad compared to the other imino protons even before the addition of the catalyst due to fraying of the end base positions; that the imino resonance for the end position is seen at all is somewhat surprising.

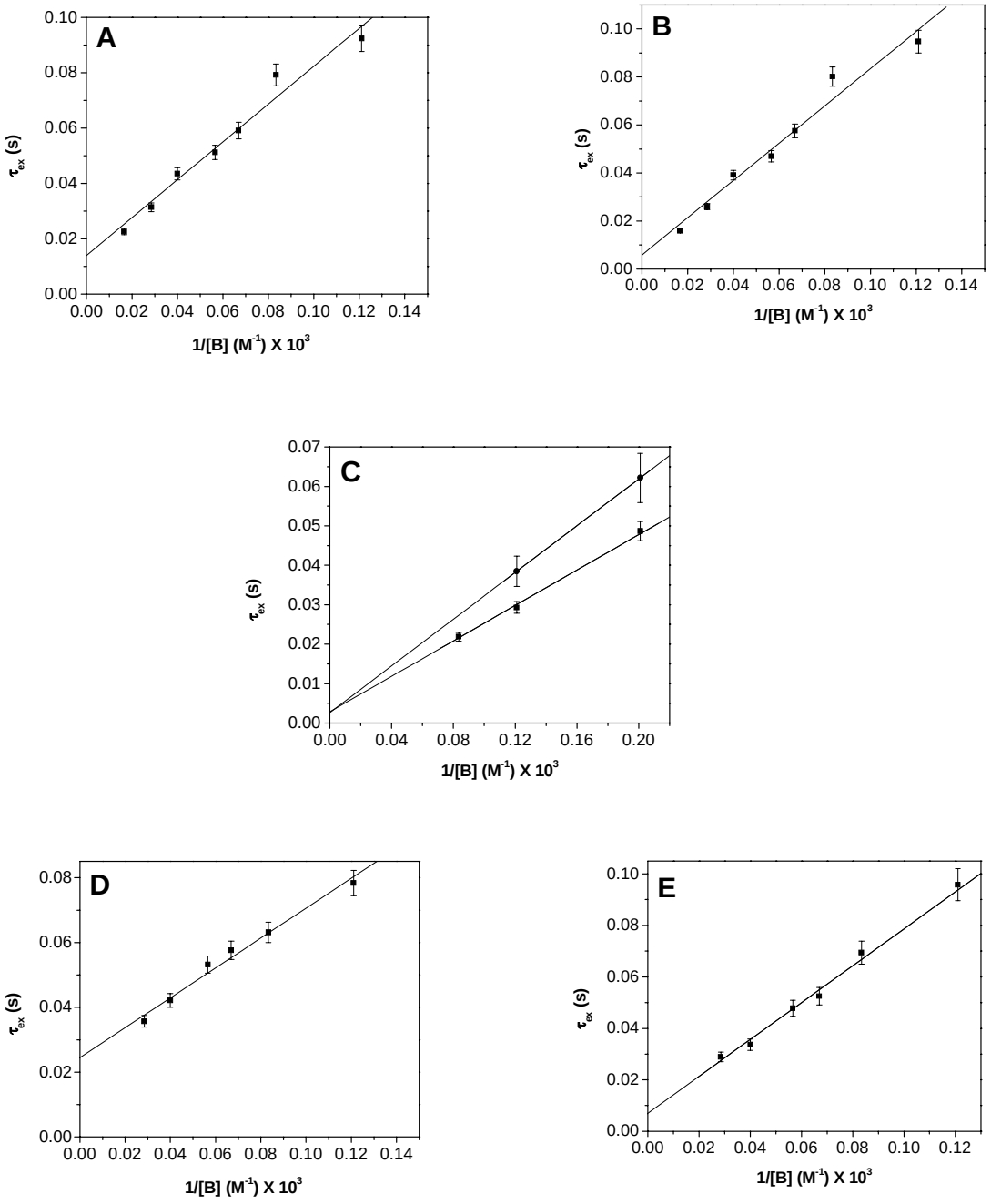

Figure 2.4. Exchange of the imino protons of the duplex d(GACAGTGTC)$_2$ containing the intervening GG mismatch versus the inverse of the concentration of ammonia catalyst. The exchange times (τ_{ex}) of (A) G7N_1H, (B) G9N_1H, (C) G5/G5'N_1H, (D) T6N_3H and (E) T8N_3H imino protons are individually displayed as a function of inverse ammonia concentration (1/[B]). The data points used in the drawing of these lines are normalized based on at least three trials. The straight lines are obtained by fitting to Equation 2, with the exchange times weighted according to their errors. The corresponding base-pair lifetimes (τ_{op}) thereby obtained from extrapolation are displayed in Table 3. Two independent line fittings are accomplished for the imino proton at the mismatch site (G5/G5'N_1H).

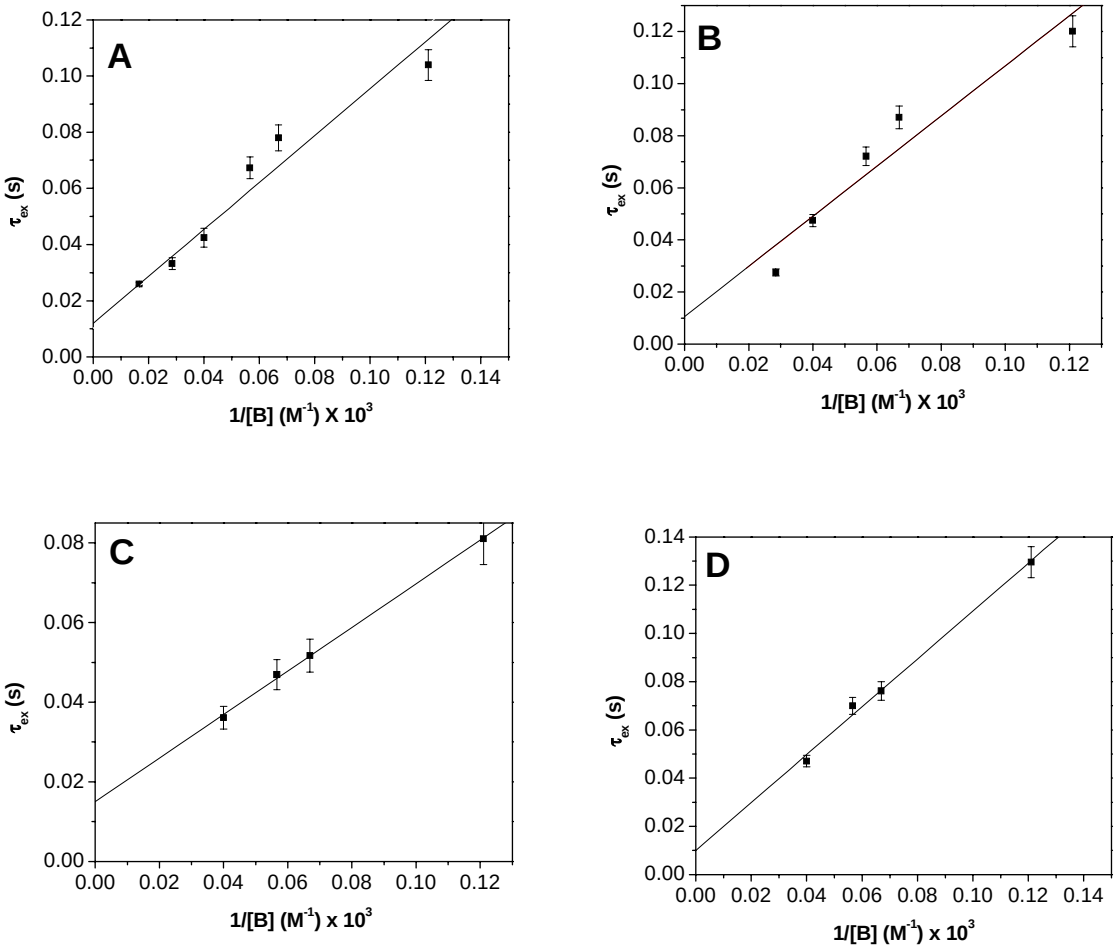

Figure 2.5. Exchange of the imino protons of the duplex d(GACAATGTC)$_2$ containing the intervening AA mismatch versus the inverse of the concentration of ammonia catalyst. The exchange times (τ_{ex}) of (A) G7NH, (B) G9NH, (C) T6NH and (D) T8NH imino protons are individually displayed as a function of inverse ammonia concentration (1/[B]). The data points used in the drawing of these lines are normalized based on at least three trials. The straight lines are obtained by fitting to Equation 2, with the exchange times weighted according to their errors. The corresponding base-pair lifetimes (τ_{op}) thereby obtained from extrapolation are displayed in Table 3.

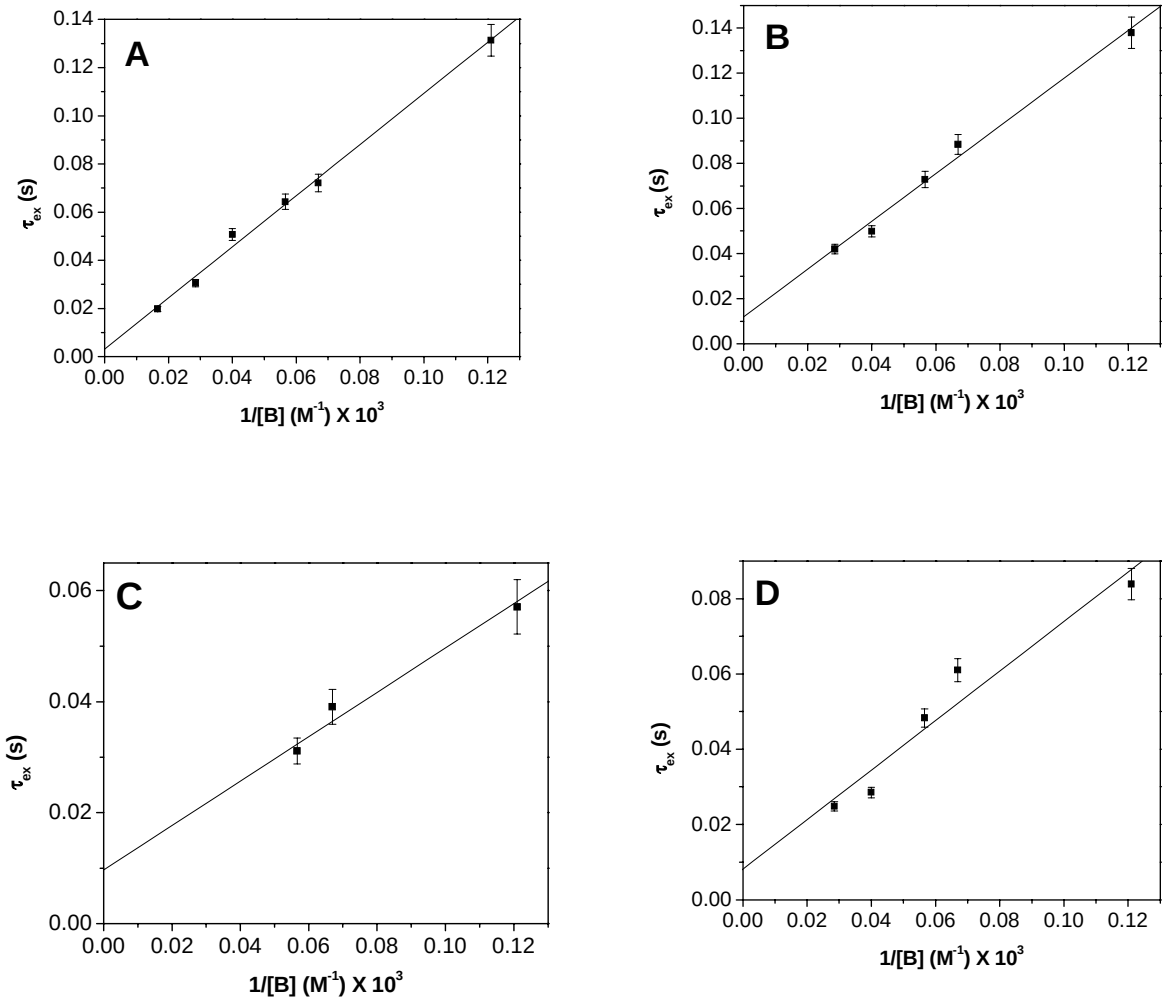

Figure 2.6. Exchange of the imino protons of the duplex d(GACA<u>C</u>TGTC)$_2$ containing the intervening CC mismatch versus the inverse of the concentration of ammonia catalyst. The exchange times (τ_{ex}) of (A) G7NH, (B) G9NH, (C) T6NH and (D) T8NH imino protons are individually displayed as a function of inverse ammonia concentration (1/[B]). The data points used in the drawing of these lines are normalized based on at least three trials. The straight lines are obtained by fitting to Equation 2, with the exchange times weighted according to their errors. The corresponding base-pair lifetimes (τ_{op}) thereby obtained from extrapolation are displayed in Table 3.

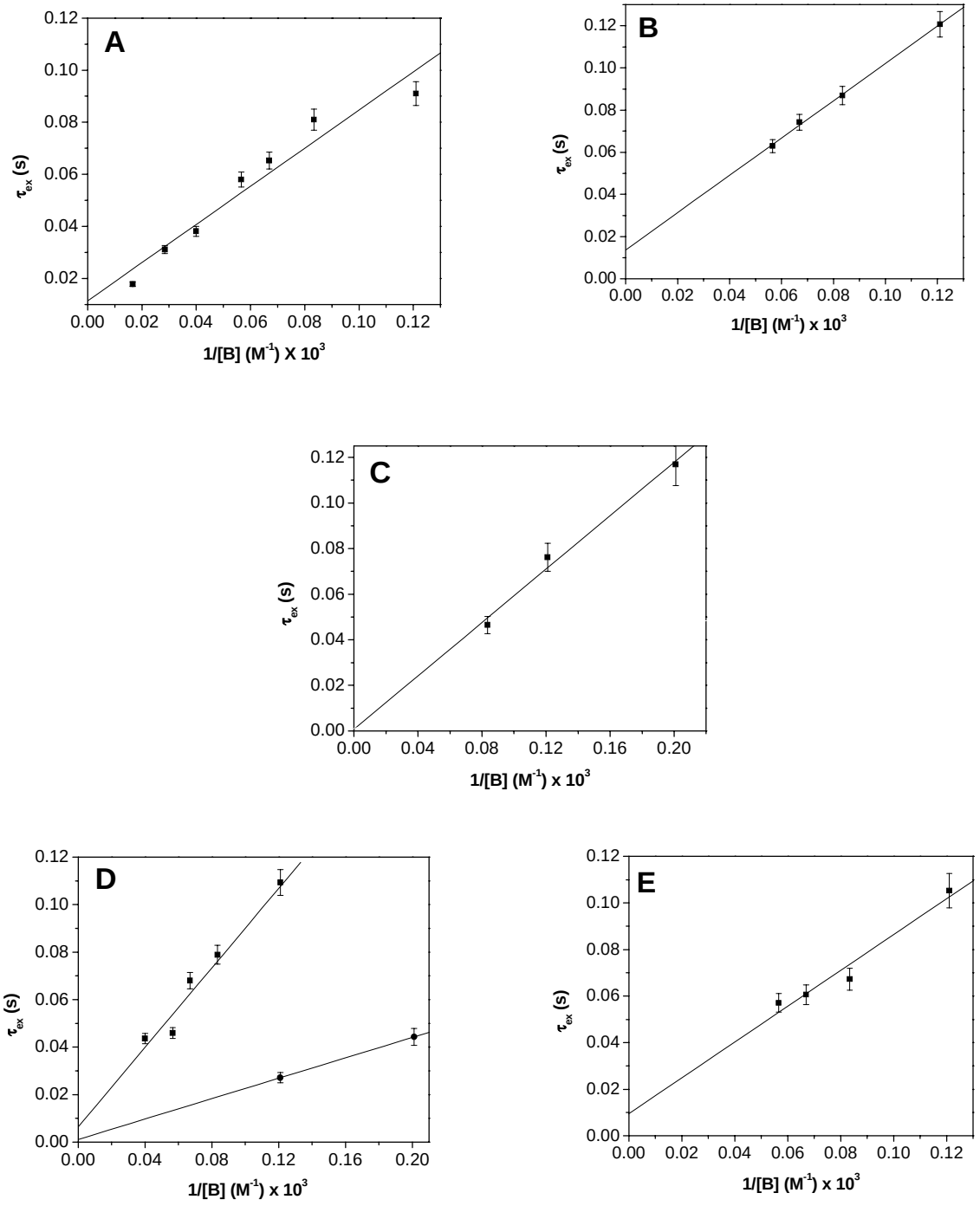

Figure 2.7. Exchange of the imino protons of the duplex d(GACA<u>T</u>TGTC)$_2$ containing the intervening TT mismatch versus the inverse of the concentration of ammonia catalyst. The exchange times (τ_{ex}) of (A) G7NH, (B) G9NH, (C) T5/T5'NH, (D) T6NH and (E) T8NH imino protons are individually displayed as a function of inverse ammonia concentration (1/[B]). The data points used in the drawing of these lines are normalized based on at least three trials. The straight lines are obtained by fitting to Equation 2, with the exchange times weighted according to their errors. The corresponding base-pair lifetimes (τ_{op}) thereby obtained from extrapolation are displayed in Table 3. In case of T6NH proton, two different lifetimes are obtained (Results & Discussion).

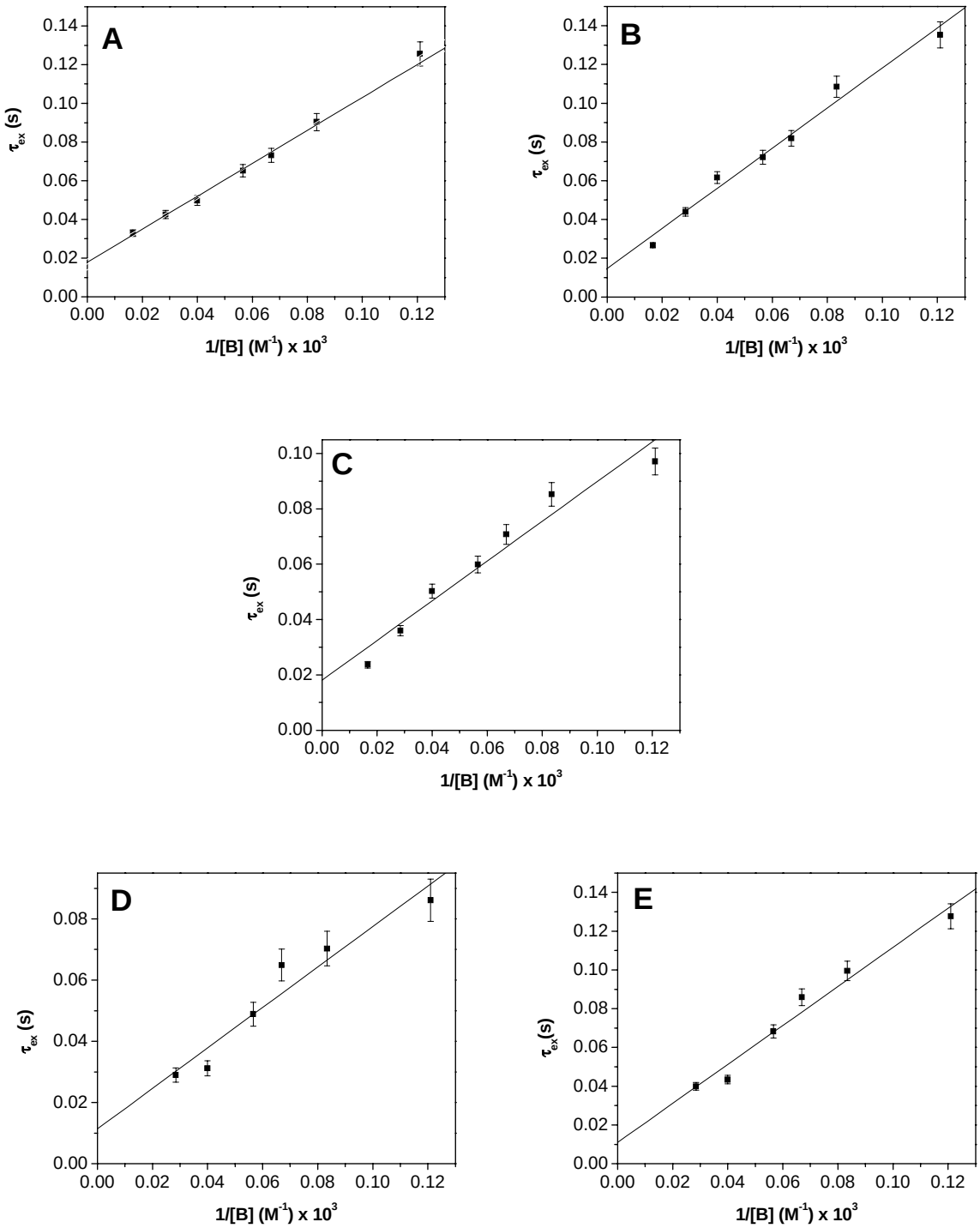

Figure 2.8. Exchange of the imino protons of the fully matched duplex d(GACAGTGTC)$_2$ versus the inverse of the concentration of ammonia catalyst. The exchange times (τ_{ex}) of (A) G7NH, (B) G9NH, (C) G5NH, (D) T6NH and (E) T8NH imino protons are individually displayed as a function of inverse ammonia concentration (1/[B]). The data points used in the drawing of these lines are normalized based on at least three trials. The straight lines are obtained by fitting to Equation 2, with the exchange times weighted according to their errors. The corresponding base-pair lifetimes (τ_{op}) thereby obtained from extrapolation are displayed in Table 3.

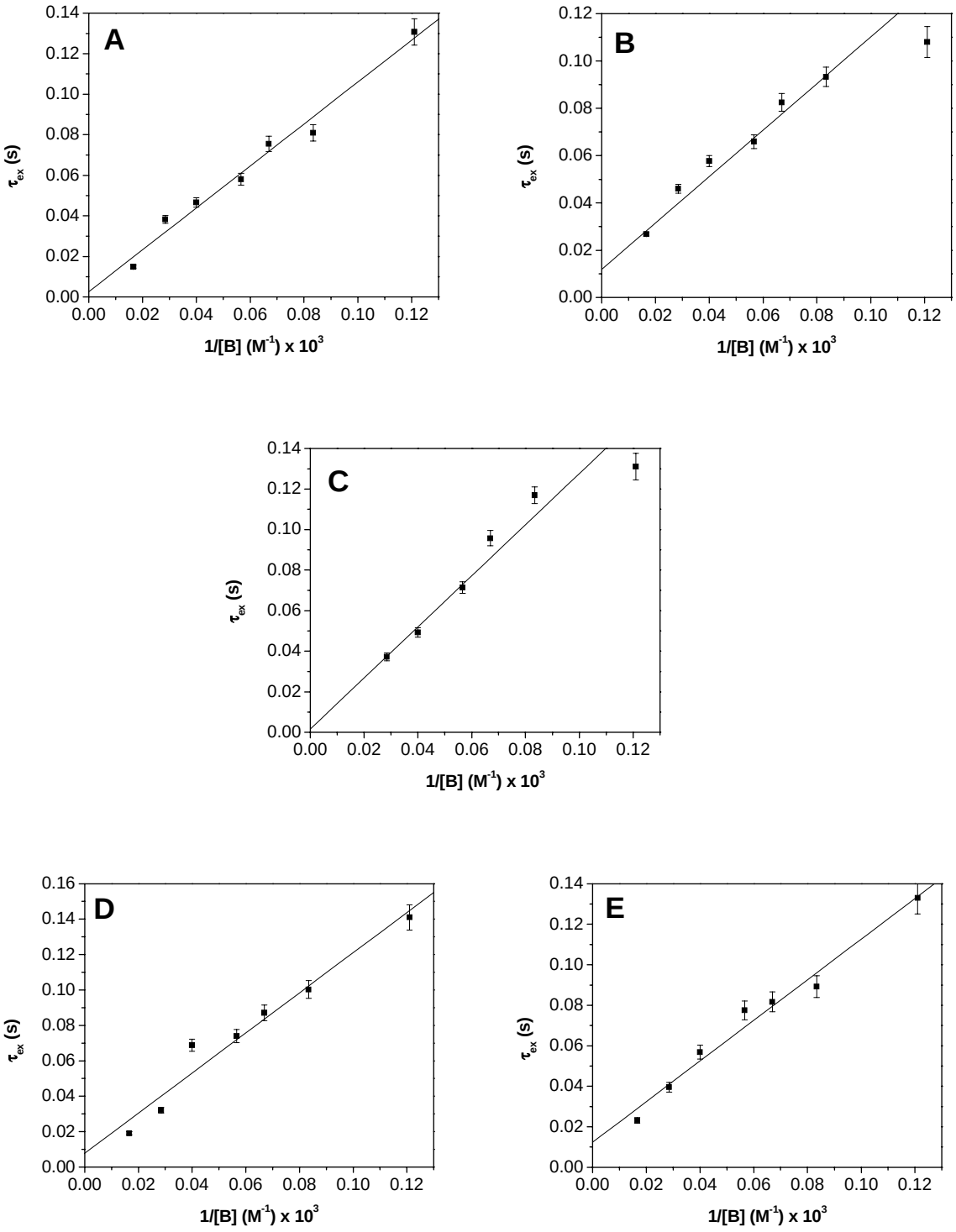

Figure 2.9. Exchange of the imino protons of the fully matched duplex d(GACAATGTC)$_2$ versus the inverse of the concentration of ammonia catalyst. The exchange times (τ_{ex}) of (A) G7NH, (B) G9NH, (C) T5NH, (D) T6NH and (E) T8NH imino protons are individually displayed as a function of inverse ammonia concentration (1/[B]). The data points used in the drawing of these lines are normalized based on at least three trials. The straight lines are obtained by fitting to Equation 2, with the exchange times weighted according to their errors. The corresponding base-pair lifetimes (τ_{op}) thereby obtained from extrapolation are displayed in Table 3.

In Figure 4, the exchange times at 277 K of the imino protons of the base pairs of the oligonucleotide containing the GG mismatch are displayed as a function of the inverse ammonia concentration. The exchange times display the linear dependence on the inverse base concentration, as expected from Equation 1. Similar plots were drawn for the other mismatches (Supporting Information) and these plots were found to be linear in all cases. Therefore, imino proton exchange in these duplexes containing single base mismatches does follow Linderstrøm-Lang kinetics (52). The base-pair lifetimes τ_{op} obtained from the linear fits are given in Table 3.

Base-pair Lifetimes. Fast exchange rates and therefore short base-pair lifetimes are observed for the imino protons directly at the mismatch sites as compared to the Watson-Crick base-pair GC (τ_{op} of $G5N_1H$ = 18±4 ms). This observation does support the fact that the mismatches produce local destabilization in the helical structure of the duplex leading to dynamics for the mismatches that are different from the standard Watson Crick base pairs. Furthermore, the τ_{op} of the GG mismatch site is, appreciably longer than that of the TT mismatch, 2 ms for $G5N_1H$ in the GG pair, while 0.5 ms for $T5N_3H$ in the case of TT. The value of τ_{op} obtained for the GG mismatch is similar to values previously reported for a GT mismatch (54).

The effect of the mismatches also propagates out to the base pairs adjacent to it, $T6N_3H$ and $G7N_1H$, such that each duplex can be distinguished by its differential kinetics. As seen in the chemical shift changes, the dynamical effects of the mismatches are mostly localized in the vicinity of the mismatch site. This finding is consistent with the crystallographic studies, that show that the conformational differences between the normal B-form and the mismatched DNA are small and affect solely the local environment of the mismatched site (10-12). This observation is also consistent with previous ^{1}H NMR studies of DNA mismatches (16, 28, 53, 54).

In fact, in the case of the duplexes containing CC and AA mismatches, the base-pair lifetime at the mismatch site clearly cannot be determined since there are no imino

Table 2.3. The Base-pair Lifetimes[a] (τ_{op}) of the Oligonucleotides Containing Intervening Mismatch (XY).

1 2 3 4 5 6 7 8 9
5'-GACAXTGTC-3' where X, Y= A, T, G, C
3'-CTGTYACAG-5'

τ_{op} (ms)[b] Base pair[c]	T5NH	G5NH	T6NH	G7NH	T8NH	G9NH
G•G[e]	X	2±1 2±0.9	24±5	15±4	8±2	7±3
T•T[f]	0.5±0.3	X	6±4 0.5±0.2	2±1	10±3	14±4
C•C[d]	X	X	10±3[g]	4±2	8±3	12±4
A•A[d]	X	X	15±3	12±3	10±2	10±4
G•C*[h]	X	18±4	12±3	18±5	11±2	15±5
A•T*[h]	1±0.4	X	8±2	3±1	12±3	12±4

[a]Samples for the determining the base-pair lifetime are prepared and the experiments based on imino proton exchange are performed as described in the Experimental section. The samples were at a concentration of 0.5-1.2 mM duplex and taken in a buffer solution of 5 mM Na_2HPO_4, 15 mM NaCl, pH 7.0 in 90:10 H_2O/D_2O. [b]Shown are the mean and standard deviation of the base-pair lifetime values (τ_{op}) of the mismatches/base-pairs (T5/G5NH) and their flanking base-pairs based on at least three trials. [c]Designation of XY as shown in assembly. [d]Since only guanine and thymine has imino protons, no base-pair lifetimes are obtained for CC and AA duplexes directly at the corresponding mismatch sites. [e]Two independent values of the base-pair lifetimes at the mismatch site are obtained for the duplexes containing GG mismatch for each trial. [f]In the case of TT mismatch, two different lifetimes are obtained for the T6NH proton (Results & Discussion). [g]The base-pair lifetime corresponding to the T6'NH of the CC mismatch could not be determined because of very fast relaxation on the addition of base. [h]XY* corresponds to the Watson-Crick paired sequence.

protons at the mismatch site to measure the relaxation times. In those cases, to compare the lifetimes with the other mismatches, the neighboring imino protons (T6 N_3H) to the mismatch site was considered.

The exchange times of T5'N_3H of the TT mismatched duplex and T6'N_3H of the CC duplex could not be determined due to very fast exchange and the rapid disappearance of the peaks on the first addition of the exchange catalyst. This observation is consistent with the very short lifetime of the TT mismatched base pair (τ_{op} = 0.5±0.3 ms) obtained independently from the other imino proton (T5N_3H) at the mismatch site. Unusually fast exchange is also observed at T6'N_3H (τ_{op} = 0.5±0.2 ms) of TT duplex, providing evidence of fast exchange occurring around the vicinity of the mismatch.

In terms of overall kinetics, the duplex containing the GG mismatch displays the longest base-pair lifetime, followed by AA, CC, and then TT with the shortest lifetime. We believe that the short base-pair lifetimes reflect an increased lateral motion of the base pair, leading to an increased disruption of the π stacked array. This disruption affects not only the imino protons at the mismatch site, but also the imino protons up to two neighboring base pairs away from the mismatch. In all of the sequences under study, the outermost GC and AT base-pairs exhibit similar values of base-pair lifetimes.

Matched Sequence. The base-pair lifetimes in the fully matched GC-containing oligonucleotide are comparable to the previously reported values for fully matched duplexes (43). However, quite contrary to our expectation, the base-pair lifetime for the AT base pair in the sequence context of 5'-A**A**T-3' was found to be much shorter than AT base pairs in other sequence contexts (43, 44) and even shorter than many mismatches (τ_{op} of T5N_3H = 1±0.4 ms). Interestingly, the flanking base pairs of the central AT base pair also show unusual rapid lifetimes as compared to the fully matched GC sequence. Note the very fast lifetime of the G7 base pair (τ_{op} of G7N_1H = 3±1 ms) in this sequence. Also note that in this given AT-duplex, different AT base pairs show different lifetimes. The one flanked by GC base pairs on both sides exhibits the longest

lifetime (τ_{op} of T8N_3H = 12±3 ms) which can be rationalized based on the fact the GC base pairs can provide better stacking for the AT base pair. It is apparent that the value of the base pair lifetimes depends upon the sequence context, as the sequence context imposes different local conformational flexibilities on the duplex DNA. These structural variations are reflected in the base pair opening dynamics.

This observation is particularly interesting because it shows that the dynamics of a fully matched base pair in a given sequence context can be comparable to a mismatched site even though this may not be reflected in the melting temperatures. Thus, an individual Watson-Crick base pair within a DNA helix may not necessarily be the most stable and well-stacked. The AT base pair in general has a longer base pair lifetime (greater than 1 ms but less than 5-6 ms) under other sequence contexts (45). In contrast, long tracts of AT base pairs show very long base pair lifetimes (greater than 100ms) (44). The alternating sequence 5'-TATA-3' is also known to be particularly flexible (40). Thus the base-pair lifetime for a given base pair depends sensitively upon the sequence context and composition. A systematic study of this effect is in progress. It is interesting to note that we have also seen evidence of the local flexibility of this sequence in studies of long-range DNA-mediated charge transport (38).

Internal Dynamics of Mismatched and Matched Base Pairs. One expects that the imino proton of a Watson-Crick base-pair (e.g., a GC pair) within a double helix cannot exchange on a rapid time scale, since neither solvent nor catalyst has access to the proton. Exchange, therefore, proceeds via three consecutive steps: base-pair opening (1), whose rate is $1/\tau_{op}$, followed by proton exchange from the open state (2) and closing the base-pair (3) (55):

$$GH^*C \leftrightarrow GH^* + C \leftrightarrow GH^{\#} + C \leftrightarrow GH^{\#}C$$

(1) (2) (3)

The base-pair lifetimes of the mismatches are found in general to be shorter than the Watson-Crick base pairs. Indeed in many cases, no "opening" of the mismatched base

pair is required. This means that the lifetime of the mismatches in the closed state is greatly reduced relative to that of the normal Watson-Crick base pairs. It has been shown (54) that ~ 0.1% of the GT mismatches are in the open solvent-accessible state and GT is one of the more thermodynamically stable mismatches. The mismatches, in general, are more accessible to solvent and other extraneous molecules than the Watson-Crick bases. This may have relevance to how the mismatches are recognized by the mismatch repairing proteins and how the mismatches may act as "hot spots" in reactivity studies (56).

The imino exchange experiments primarily measure the lateral motions of the base pairs. These opening motions may occur by different pathways and may be coupled to bending (57-60) which in turn affects the stacking of the base-pairs. Stacking is mostly a "vertical" effect along the axis of the duplex while the opening motions are "horizontal" effects. However, these two are clearly related, possibly one motion reinforcing the other. Molecular dynamics (MD) simulations have been performed on the lateral motion of duplexes containing mismatches (61). Consistent with the short lifetime of mismatches, opening fluctuations in MD runs are larger at mismatched base-pairs 5-7°, than fully matched CG, 4°. It should however be emphasized that by measuring the base-pair lifetime, we are essentially quantifying only one type of dynamical motion occurring in the DNA duplex. Mismatches can bring about changes in a variety of other internal motions in DNA like helical twisting, propeller twisting, base tilting, base rolling etc and these internal motions are not reflected in the study of base-pair lifetimes, although they may be related.

Conclusions

A systematic study of the base-pair dynamics of mismatch containing oligonucleotides has been carried out using imino exchange measurements. We have observed very fast base-pair opening rates in the mismatch site, indicative of the local

distortion generated around the mismatch. Some mismatches generate more distortion than others, and these differences are captured in the faster base-pair lifetimes. A relative ordering of the mismatches with respect to the base-pair lifetime has been achieved. In general, the mismatches are found to be kinetically destabilized relative to the Watson Crick base-pairs. However, certain Watson-Crick base-pairs under a given sequence context may behave very much like a mismatch in terms of base-pair opening dynamics. The faster dynamics associated with the mismatches and with some Watson- Crick base pairs requires consideration in how these sites may be recognized and repaired by proteins.

Acknowledgements

We are grateful to the National Institutes of Health (GM33309) for their financial support of this work. We also thank Dr. Scott Ross and Helen Chuang, a summer undergraduate research fellow for technical assistance.

References

1. Goodman, M. F., Creighton, S., Bloom, L. B., and Petruska, J. (1993) Biochemical basis of DNA-replication fidelity. *Crit. Rev. Biochem. Mol. Biol.,* **28**, 83-126.
2. Bhattacharyya, A. (1989) Single base mismatches in DNA- long-range and short-range structure probed by analysis of axis trajectory and local chemical-reactivity. *J. Mol. Biol.,* **209**, 583-597.
3. Leonard, G. A., Booth, E. D., and Brown, T. (1990) Structural and thermodynamic studies on the adenine guanine mismatch in B-DNA. *Nucleic Acids Res.,* **18**, 5617-5623.
4. Plum, G. E., Grollman, A. P., Johnson, F., and Breslauer, K. J. (1995) Influence of the oxidatively damaged adduct 8-oxodeoxyguanosine on the conformation, energetics, and thermodynamic stability of a DNA duplex. *Biochemistry,* 3**4**, 16148-16160.
5. Brown, T. (1995) Mismatches and mutagenic lesions in nucleic acids. *Aldrichimica Acta,* **28**, 15-20.
6. Lindahl, T. (1993) Instability and decay of the primary structure of DNA. *Nature,* **362**, 709-715.
7. Rajski, S. R., Jackson, B. A., and Barton, J. K. (2000) DNA repair: models for damage and mismatch recognition. *Mut. Res.,* **447**, 49-72.
8. Kolodner, R. (1996) Biochemistry and genetics of eukaryotic mismatch repair. *Genes Dev.,* **10**, 1433-1442.
9. Modrich, P. (1991) Mechanisms and biological effects of mismatch repair. *Annu. Rev. Genet.,* **25**, 229-253.
10. Brown, T., Kennard, O., Kneale, G., and Rabinovich, D. (1985) High-resolution structure of a DNA helix containing mismatched base-pairs. *Nature,* **315**, 604.

11. Hunter, W. N., Brown, T., Kneale, G., Anand, N. N., Rabinovich, D., and Kennard, O. (1987) The structure of guanosine-thymidine mismatches in B-DNA at 2.5 Å resolution. *J. Bio. Chem.,* **262**, 9962.

12. Hunter, W. N., Brown, T., and Kennard, O. (1987) Structural features and hydration of a dodecamer duplex containing two CA mispairs. *Nucleic Acids Res.,* **15**, 6589-6606.

13. Sowers, L. C., Fazakerley, G. V., Eritja, R., Kaplan, B. E., and Goodman, M.F. (1986) Base-pairing and mutagenesis-observation of a protonated base pair between 2-aminopurine and cytosine in an oligonucleotide by proton NMR. *Proc. Natl. Acad. Sci. USA*, **83**, 5434-5438.

14. Fazakerley, G. V., Quignard, E., Woisard, A., Guschlbauer, W., Vandermarbel, G. A., Vanboom, J. H., Jones, M., and Radman, M. (1986) Structures of mismatched base pairs in DNA and their recognition by the Escherichia coli mismatch repair system. *EMBO J.*, **5**, 3697-3703.

15. Fazakerley, G. V., Sowers, L. C., Eritja, R., Kaplan, B. E., and Goodman, M.F. (1987) NMR-studies on an oligodeoxynucleotide containing 2-aminopurine opposite adenine. *Biochemistry*, **28**, 5641-5646.

16. Patel, D. J., Kozlowski, S. A., Ikuta, S., and Itakura, K. (1984) Deoxyadenosine pairing in the d (CGAGAATTCGCG) duplex-conformation and dynamics at and adjacent to the dG.dA mismatch site. *Biochemistry,* **23**, 3207-3217.

17. Faibis, V., Cognet, J. A. H., Boulard, Y., Sowers, L. C., and Fazakerley, G. V. (1996) Solution structure of two mismatches G·G and I·I in the K-*ras* gene context by nuclear magnetic resonance and molecular dynamics. *Biochemistry,* **35**, 14452.

18. Borden, K. L. B., Jenkins, T. C., Skelly, J. V., Brown, T., and Lane, A. N. (1992) Conformational properties of the G·G mismatch in d(CGCGAATTGGCG)$_2$ determined by NMR. *Biochemistry,* **31**, 5411-5422.

19. Cognet, J. A. H., Gabarro-Arpa, J., LeBret, M., Van der Marel, G. A., Boom J. H., and Fazakerley, G. V. (1991) Solution conformation of an oligonucleotide containing a G.G mismatch determined by nuclear magnetic resonance and molecular mechanics. *Nucleic Acids Res.,* **19**, 6771-6779.

20. Gervais, V., Cognet, J. A. H., LeBret, M., Sowers, L. C., and Fazakerley G. V. (1995) Solution Structure of two mismatches A·A and T·T in the K-*ras* gene context by nuclear magnetic resonance and molecular dynamics. *Eur. J. Biochem.*, **228**, 279-290.

21. Maskos, K., Gunn, B. M., LeBlanc, D. A., and Morden, K. M. (1993) NMR study of G.A and A.A pairing in d(GCGAATAAGCG)$_2$. *Biochemistry* **32**, 3583-3595.

22. Arnold, F. H., Wolk, S., Cruz, P., and Tinoco, I. J. (1987) Structure, dynamics, and thermodynamics of mismatched DNA oligonucleotide duplexes d(CCCAGGG)$_2$ and d(CCCTGGG)$_2$. *Biochemistry,* **26**, 4068-4075.

23. Boulard, Y., Cognet, J. A. H., and Fazakerley, G. V. (1997) Solution structure as a function of pH of two central mismatches, C·T and C·C, in the 29 to 39 K- *ras* gene sequence, by nuclear magnetic resonance and molecular dynamics. *J. Mol. Biol.*, **268**, 331-347.

24. Peyret, P., Seneviratne, A., Allawi, H. T., and SantaLucia, Jr, J. (1999) Nearest-neighbor thermodynamics and NMR of DNA sequences with internal A·A, C·C, G·G, and T·T mismatches. *Biochemistry*, **38**, 3468-3477

25. Greene, K. L., Jones, R. L., Li, Y., Robinson, H., Howard, W., Andrew, H. J., Zon, G., and Wilson, W. D. (1994) Solution Structure of G·A mismatch DNA sequence d(CCATGAATGG)$_2$, determined by 2D NMR and structural refinement methods. *Biochemistry,* **33**, 1053-1062.

26. Gao, X., and Patel, D. J. (1988) G(syn).A(anti) mismatch formation in DNA dodecamers at acidic pH; pH -dependent conformational transition of G.A mispairs detected by proton NMR. *J. Am. Chem. Soc.*, **110**, 5178-5182.

27. Cheng, J. W., Chou, S. H., and Reid, B. R. (1992) Solution Structure of d(ATGAGCGAATA)2 - adjacent G·A mismatches stabilized by cross-strand base-stacking and B(II) phosphate groups. *J. Mol. Biol.*, **228**, 138-155.

28. Li, Y., Gerald, W., and David, W. (1991) Thermodynamics of DNA duplexes with adjacent G.A mismatches. *Biochemistry*, **30**, 7566-7572.

29. Allawi, H. T., and SantaLucia, Jr, J. (1998) NMR solution structure of a DNA dodecamer containing single G·T mismatches. *Nucleic Acids Res.*, **26**, 4925-4934.

30. Boon, E. M., Ceres, D. M., Drummond, T. G., Hill, M. G., and Barton, J. K. (2000) Mutation detection by electrocatalysis at DNA-modified electrodes. *Nature Biotechnology*, **18**, 1096.

31. Williams, T. T., Odom, D. T., and Barton, J. K. (2000) Variations in DNA charge transport with nucleotide composition and sequence. *J. Am. Chem. Soc.*, **122**, 9048-9049.

32. Kelley, S. O., Boon, E. M., Barton, J. K., Jackson, N. M., and Hill, M. G. (1999) Single-base mismatch detection based on charge transduction through DNA. *Nucleic Acids Res.*, **27**, 4830.

33. Lewis, F. D., R. L. Letsinger, M. R. Wasielewski, (2001) Dynamics of photoinduced charge transfer and hole transport in synthetic DNA hairpins. *Acc. Chem. Res.*, **34**, 159-170.

34. Kelley, S. O., Jackson, N. M., Hill, M. G., and Barton, J. K. (1999) Long range electron transfer through DNA films. *Angew. Chem. Int. Ed. Engl.*, **38**, 941.

35. Boon, E. M. and Barton, J. K. (2002) Charge transport in DNA. *Current Opin. Structural Biol.*, **12**, 320-329.

36. Giese, B. (2000) Long distance charge transport in DNA: The hopping mechanism. *Acc. Chem. Res.*, **33,** 631-636.

37. Schuster, G. B. (2000) Long-range charge transfer in DNA: Transient structural distortions control the distance dependence. *Acc. Chem. Res.*, **33**, 253-260.

38. Bhattacharya, P. K., and Barton, J. K. (2001) The influence of intervening mismatches on long-range guanine oxidation in DNA duplexes. *J. Am. Chem. Soc.*, **123**, 8649 -8656.

39. Guest, C. R., Hochstrasser, R. A., Sowers, L. C., and Millar, D. P. (1991) Dynamics of mismatched base-pairs in DNA. *Biochemistry,* **30**, 3271-3279.

40. Dickerson, R.E. (1998) Structure, Motion, Interaction and Expression of Biological Macromolecules. Sarma, R. H. and Sarma, M. H. (eds.), *Proceedings of Tenth Conversations in Biomolecular Stereodynamics.* Adenine Press, Schenectady, NY., pp. 17-36.

41. Englander, S. W., and Kallenbach, N. R. (1983) Hydrogen exchange and structural dynamics of proteins and nucleic acids. *Q. Rev. Biophys.*, **16**, 521-655.

42. Nonin, S., Leroy, J. L., and Gueron, M. (1995) Terminal base pairs of oligodeoxynucleotides: imino proton exchange and fraying. *Biochemistry,* **34**, 10652-10659.

43. Gueron, M., and Leroy, J. L. (1992) Base-pair opening in double-stranded nucleic acids**.** Eckstein, F. and Lilley, D. M. J. (eds), *Nucleic Acids and Molecular Biology*. Springer-Verlag Berlin Heidelberg, Vol 6, pp. 1-22.

44. Leroy, J. L., Charretier, E., Kochoyan, M., and Guéron, M. (1988) Evidence from base-pair kinetics for two types of adenine tract structures in solution-their relation to DNA curvature. *Biochemistry,* **27**, 8894-8898.

45. Dornberger, U., Leijon, M., and Fritzsche, H. (1999) High base pair opening rates in tracts of GC base pairs. *J. Biol. Chem.*, **274**, 6957-6962.

46. Leijon, M., Sehlstedt, U., Nielsen, P. E., and Gräslund, A. (1997) Unique base-pair breathing dynamics in PNA-DNA hybrids. *J. Mol. Biol.* **271**, 438-455.

47. Leroy, J. L., Gao, X. L., Guéron, M., and Patel, D. J. (1991) Proton-exchange and internal motions in two chromomycin dimer DNA oligomer complexes. *Biochemistry,* **30**, 5653-5661.

48. Caruthers, M. H., Barone, A. D., Beaucage, S. L., Dodds, D. R., Fisher, E.F., McBride, L.J., Matteucci, M., Stabinsky, Z., and Tang, J.Y. (1987) Chemical synthesis of deoxyoligonucleotides by the phosphoramidite method. *Meth. Enzymol.* **154**, 287-313.

49. Piotto, M., Saudek, V., and Sklenar, V. J. (1992) Gradient-tailored excitation for single-quantum NMR spectroscopy of aqueous-solutions. *Biomol. NMR* **2**, 661-665.

50. Maltseva, T. V., Yamakage, S. I., and Chattopadhyaya, J. (1993) Direct estimation of base-pair exchange kinetics in oligo-DNA by a combination of NOESY and ROESY experiments. *Nucleic Acids Res.* **18**, 4288-4295.

51. Hwang, T. L., and Shaka, A. J. (1992) Cross relaxation without TOCSY- transverse rotating frame overhauser effect spectroscopy. *J. Am. Chem. Soc.* **114**, 3157-3159.

52. Hvidt, A., and Nielsen, S. O. (1966) Hydrogen exchange in proteins. *Adv. Protein Chem.*, **21**, 287-386.

53. Pardi, A., Morden, K. M., and Patel, D. J. (1982) Kinetics for exchange of imino protons in the d(CGCGAATTCGCG) double helix and in two similar helices that contain a G-T base pair, d(CGTGAATTCGCG), and an extra adenine, d(CGCAGAATTCGCG). *Biochemistry,* **21**, 6567-6574.

54. Moe, J. G., and Russu, I. M. (1992) Kinetics and energetics of base-pair opening in 5'-d(CGCGAATTCGCG)-3' and a substituted dodecamer containing G.T mismatches. *Biochemistry*, **31**, 8421-8428.

55. Gueron, M., and Leroy, J. L. (1995) Studies of base pair kinetics by NMR measurement of proton exchange. *Methods Enzymol.*, **261**, 383-413.

56. Arkin, M. R., Stemp, E. D. A., and Barton, J. K. (1997) Long-range oxidation of guanine by Ru(III) in duplex DNA. *Chem. Biol.*, **4**, 389.

57. Keepers, J., Kollman, P. A., Weiner, P. K., and James, T. L. (1982) Molecular mechanical studies of DNA flexibility coupled backbone torsion angles and base-pair openings. *Proc. Natl. Acad. Sci. USA*, **79**, 5537-5541.

58. Keepers, J., Kollman, P. A., and James, T. L. (1984) Molecular mechanical studies of base-pair opening in d(CGCGC)-d(GCGCG), dG5.dC5, d(TATAT)-d(ATATA), and dA5.dT5 in the B-form and Z-form of DNA. *Biopolymers*, **23**, 2499-2511.

59. Ramstein, J., and Lavery, R. (1988) Energetic coupling between DNA bending and base pair opening. *Proc. Natl. Acad. Sci. USA*, **85**, 7231-7235.

60. Ramstein, J., and Lavery, R. (1990) Base pair opening pathways in B-DNA. *J. Biomol. Struct. Dynam.*, **7**, 915-933.

61. Cognet, J. A. H., Boulard, Y., and Fazakerley, G. V. (1995) Helical parameters, fluctuations, alternative hydrogen-bonding, and bending in oligonucleotides containing a mismatched base-pair by NOESY distance restrained and distance free molecular dynamics. *J. Mol. Biol.*, **246**, 209-226.